Sm_2Fe_{17} and Tm_2Fe_{17}: electronic structure, magnetic and optical properties

2007 J. Phys.: Condens. Matter 19 116215

(http://iopscience.iop.org/0953-8984/19/11/116215)

IOP PUBLISHING JOURNAL OF PHYSICS: CONDENSED MATTER

J. Phys.: Condens. Matter **19** (2007) 116215 (10pp) doi:10.1088/0953-8984/19/11/116215

Sm_2Fe_{17} and Tm_2Fe_{17}: electronic structure, magnetic and optical properties

Yu V Knyazev[1], Yu I Kuz'min[1], A G Kuchin[1], A V Lukoyanov[2] and I A Nekrasov[3]

[1] Institute of Metal Physics, Russian Academy of Sciences, Ural Division, 620041 Ekaterinburg, Russia
[2] Ural State Technical University—UPI, 620002 Ekaterinburg, Russia
[3] Institute of Electrophysics, Russian Academy of Sciences, Ural Division, 620049 Ekaterinburg, Russia

E-mail: knyazev@imp.uran.ru

Received 5 December 2006, in final form 15 February 2007
Published 5 March 2007
Online at stacks.iop.org/JPhysCM/19/116215

Abstract

For two intermetallics, the results of experimental measurements of optical and magnetic properties together with calculations in the frame of the LSDA + U method are reported. The calculations of the electronic structure allow one to interpret the curves of optical conductivity extracted from direct experimental ellipsometry measurements of optical constants. A detailed analysis shows that, whereas experimental curves of the optical conductivity for both compounds are similar to each other, the contributions of various interband transitions are slightly different. Also band structure calculations give magnetic structure and values of magnetic moments for each ion in Sm_2Fe_{17} and Tm_2Fe_{17} as well as the total one in good agreement with experimental values if the orbital moment is taken into account. Obtained optical theoretical and experimental results demonstrate good agreement with each other for both intermetallics.

(Some figures in this article are in colour only in the electronic version)

1. Introduction

Intermetallic compounds of rare-earth (R) and transition-metal (T) atoms attract attention both for the technological application and from the viewpoint of basic research [1, 2]. Some of these materials exhibit large uniaxial magnetocrystalline anisotropy, high saturation magnetization and high Curie temperature (T_C) [2]. Also, the R–T intermetallics are relevant to the electron theory, because their properties mainly result from an interplay between localized rare-earth 4f states, itinerant transition-metal 3d and rare-earth 5d states [3]. The iron-rich R_2Fe_{17} compounds have large magnetic moments, but a comparatively low T_C [2]. During recent years much progress has been made in understanding the means to increase the Curie

temperature of the materials. These studies have centred on the changes in the electronic and magnetic properties which result from either substituting other elements into R_2Fe_{17} [4–7] or preparing materials with additional atoms located interstitially [8–11] or by means of both these methods [12]. For instance, magnetic properties of Sm_2Fe_{17} can be improved substantially by introducing interstitial nitrogen, e.g., $Sm_2Fe_{17}N_{3-\delta}$ [9, 10]. Compared to the parent compound, the Curie temperature of the nitride is doubled to 749 K. Improvement of the intrinsic magnetic properties of Sm_2Fe_{17} can also be achieved with interstitial carbon [11] and simultaneous partial substitution of Fe by Al, Ga or Co [12]. The primary mechanism for the drastic change of T_C in the R–Fe compounds with interstitial addition and substitution modification was investigated theoretically using a mean-field model and an interatomic-distance dependent exchange energy [8, 10, 13, 14]. Although this model correlates with the experimental results of T_C increasing in a wide variety of the compounds, there are several that exhibit a contradiction. Also, the Curie temperature variability in such systems has been explained with the spin-fluctuation theory of the Mohn–Wohlfarth approach [15], which relates the electronic structure to T_C. In this way the relative changes in T_C upon interstitial and substitution modifications of a number of R_2Fe_{17} compounds have been qualitatively explained [7] or calculated, in good agreement with experiment [16–18]. But the pure R_2Fe_{17} compounds have not been understood thoroughly; to do this in this paper we address pure Sm_2Fe_{17} and Tm_2Fe_{17} intermetallics themselves without any impurities or substitutions.

These unusual properties stimulated experimental and theoretical studies, especially investigations of the electronic structure and related properties of R_2Fe_{17}. Experimental studies were performed on the low-temperature specific heat [7] and optical properties [7, 19–22], x-ray absorption [23, 24], Mössbauer [25, 26] and photoemission [17] spectra. Electronic structure, local magnetic moments, crystal-field parameters, optical absorption and other characteristics have been calculated for some parent compounds [16, 18, 21, 22] and pseudobinary alloys [16, 18, 27, 28] by the *ab initio* band theory in the local spin-density approximation (LSDA). Recently, one more step forward to a thorough investigation of the intermetallics was taken within the local spin-density approximation with the Coulomb correction (LSDA + U) for strong electron–electron correlations in the 4f shell of rare-earth elements for Pr_2Fe_{17} and Gd_2Fe_{17} [22]. This paper continues this research for two more intermetallics and presents the theoretical calculations of the electronic properties of Sm_2Fe_{17} and Tm_2Fe_{17} together with experimental magnetic and optical measurements.

The paper is organized in the following way. In section 2 we briefly describe experimental details and results for Sm_2Fe_{17} and Tm_2Fe_{17}. Section 2.1 is devoted to sample preparation, x-ray-diffraction structural analysis and magnetic measurement conditions. Section 2.2 contains a description of the optical experiments. The results of the electronic structure calculations and magnetic properties by the LSDA + U method for these compounds are contained in section 3. The detailed analysis of optical conductivity is presented in section 4. Finally, we summarize the main results of the paper in section 5.

2. Experiment

2.1. Samples and magnetic measurements

The alloys under study were prepared by induction melting in alumina crucibles under argon atmosphere. The ingots were homogenized in the high-purity argon atmosphere at ∼1400–1450 K. According to x-ray diffraction analysis the alloys were single phase and have a rhombohedral structure of the Th_2Zn_{17} type (space group $R\bar{3}m$) for Sm_2Fe_{17} and hexagonal crystal structure of the Th_2Ni_{17} type (space group $P6_3/mmc$) for Tm_2Fe_{17}. The lattice

Table 1. Experimental parameters of Sm_2Fe_{17} and Tm_2Fe_{17}: lattice parameters a and c; unit-cell volume V at room temperature; T_C—Curie temperature; M_s—spontaneous magnetization at $T = 4$ K; relaxation γ and plasma Ω frequencies; N_{eff}—effective concentration of conduction electrons.

Compound	a (Å)	c (Å)	V (Å^3)	T_C (K)	M_s (μ_B/f.u.)	γ (10^{14} s^{-1})	Ω^2 (10^{30} s^{-2})	N_{eff} (10^{22} cm^{-3})
Sm_2Fe_{17}	8.552	12.442	788.1	393	33.1	1.8	20.6	0.65
Tm_2Fe_{17}	8.406	8.284	506.9	280[a]	20.4	1.4	17.3	0.55

[a] The Néel temperature T_N.

parameters at room temperature are shown in table 1. Sm_2Fe_{17} is a collinear ferromagnet, whereas Tm_2Fe_{17} is a collinear ferrimagnet at low T and a helical antiferromagnet at high T [2]. The spontaneous magnetization of Sm_2Fe_{17} at $T = 4$ K was determined from the magnetization curve measured on isotropic and aligned powders with particle sizes < 0.05 mm with the help of a vibrating sample magnetometer in fields up to 90 kOe. The Curie point of the Sm_2Fe_{17} compound was determined from the temperature dependences of ac susceptibility. The ac susceptibility was measured by a differential method in an ac magnetic field of 8 Oe with a frequency of 80 Hz. The ingot of Tm_2Fe_{17} was coarse grained and it was possible to cut from it spherical single crystals 0.5–1 mm in diameter. Magnetic properties of the Tm_2Fe_{17} compound were studied on a single-crystalline sample using a SQUID magnetometer in the temperature range 4–300 K and at magnetic fields up to 50 kOe. Tm_2Fe_{17} is the unique compound among the R_2Fe_{17} series having magnetocrystalline anisotropy of an easy-axis type at low temperature. At T higher than 72 K a spin orientation transition from the hexagonal c axis to the (001) plane takes place, then at T about 245 K the ferromagnet transforms to the helical antiferromagnet with the Néel temperature $T_N = 280$ K. All these magnetic transformations with temperature variation were studied from temperature dependences of magnetization in a field of 0.1 kOe. The spontaneous magnetization of Tm_2Fe_{17} at $T = 4$ K was determined from the magnetization curve measured along the c axis. The preliminary orientation of the single crystal was set by the x-ray method. The structural and magnetic parameters of the compounds are listed in table 1. They somewhat differ from previously reported data [29], most probably, because of some deviations of the samples from stoichiometry and measurements up to higher fields. For the optical studies the specular surface of the samples was prepared by mechanical polishing with diamond powders.

2.2. Optical measurements

The optical properties of Sm_2Fe_{17} and Tm_2Fe_{17} were investigated using the ellipsometric Beattie method [30]. Spectroscopic ellipsometry is based on the fact that the state of polarization of incident light is changed on reflection. This change is directly related to the dielectric function of the reflecting material. The optical constants—refractive index n and absorption coefficient k—were measured over the spectral interval from 0.827 to 5.64 eV at room temperature. The optical parameters in the short-wave range 5.6–8.5 eV were obtained from reflectivity spectra by the Kramers–Kronig transformation. The values of n and k were used to calculate the real $\epsilon_1 = n^2 - k^2$ and imaginary $\epsilon_2 = 2nk$ parts of the complex permittivity, reflectivity $R = [(n-1)^2 + k^2]/[(n+1)^2 + k^2]$ and the optical conductivity $\sigma = nk\omega/2\pi$, where ω is the angular frequency of the light wave.

The dependences of n, k, ϵ_1, ϵ_2 and R versus photon energy E for the Sm and Tm compounds are shown in figure 1. The close resemblance of these parameters for both materials attracts attention. In the whole spectral interval the magnitudes of k exceed the values of

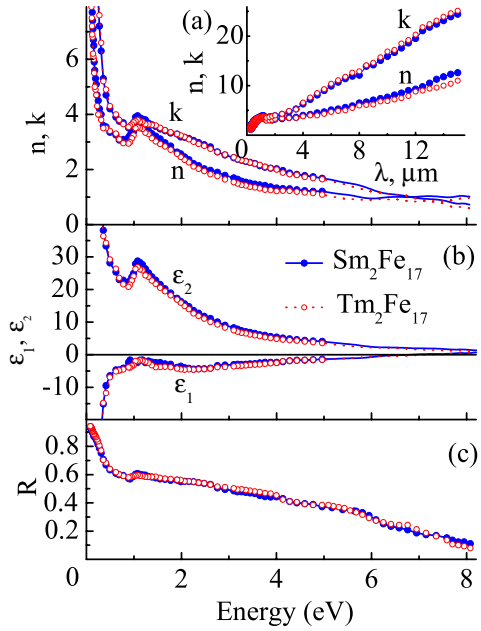

Figure 1. Experimental optical constants n and k (a), dielectric functions ϵ_1 and ϵ_2 (b) and reflectivity spectra R (c) for Sm_2Fe_{17} (full circles and solid line) and Tm_2Fe_{17} (empty circles and dotted line) compounds. Dotted and solid lines above 5 eV represent values obtained by the Kramers–Kronig transformation from reflection spectra. The inset presents dependences of the optical constants on wavelength for an expanded view in the infrared region.

n that are typical for metal-like solids. The optical responses of metallic surfaces involve contributions from both intraband and interband transitions. The intraband (Drude) contribution to the dielectric function is usually dominant for photon energies below about 1 eV, while at higher photon energy the dielectric function is dominated by interband transitions. With the increase of the wavelength to infrared region quantities n and k grows (inset of figure 1(a)). Such a character of the frequency dependences of the optical constants leads to negative quantities ϵ_1. From the spectral profile of $\epsilon_2(E)$ one finds a strong absorption band above 1 eV. As follows from the dispersion of $R(E)$, in the infrared range the reflectance exhibits high values. It is seen from figure 1 that below ∼0.5 eV the $\epsilon_1(E)$ and $\epsilon_2(E)$ spectra for both investigated compounds are Drude-like and correspond to the intraband absorption. Frequency dependences of these parameters according to such an approximation can by expressed as $\epsilon_1 = 1 - \Omega^2/(\omega^2 + \gamma^2)$ and $\epsilon_2 = \Omega^2\gamma/\omega(\omega^2 + \gamma^2)$, where Ω and γ are the plasma and effective relaxation frequencies of free charge carriers. The values of Ω and γ determined from these relations are practically unchanged in the long-wave region and were used to estimate the charge-carrier concentration $N = \Omega^2 m/4\pi e^2$ (m and e are the mass and the charge of a free electron, respectively). All these electronic parameters are shown in table 1.

Figure 2 presents the optical conductivities $\sigma(\omega)$ for both compounds. Above the energy of 0.5 eV these spectra show the intensive maxima of interband absorption. The structure of the observed maxima is asymmetrical with an abrupt low-energy edge and a smooth diminishing high-energy side with minor features at 3–4 eV. Similar behaviour of $\sigma(\omega)$ curves, caused by the high content of iron, was observed earlier in other R_2Fe_{17} compounds [19–22]. In the infrared range the optical conductivities show a rapid growth that is a typical manifestation of the predominance of the intraband absorption.

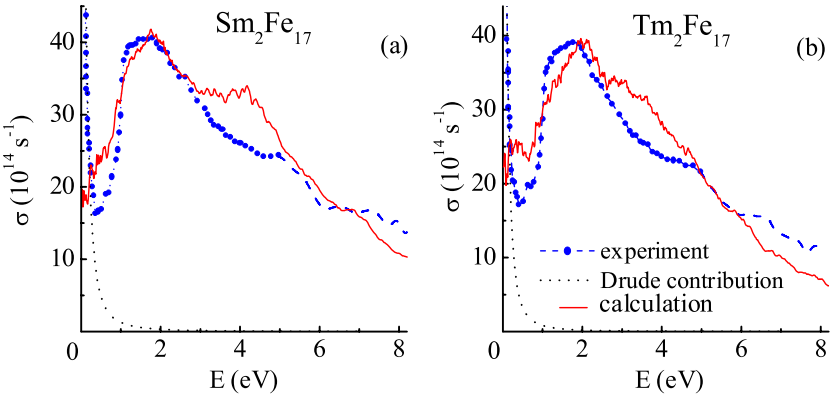

Figure 2. Experimental (dark circles and dashed lines) and calculated (solid lines) dispersion dependences of optical conductivity for Sm_2Fe_{17} (a) and Tm_2Fe_{17} (b) compounds. Dashed lines represent $\sigma(\omega)$ values obtained by the Kramers–Kronig transformation from reflection spectra. Dotted lines correspond to intraband contributions estimated by the Drude formula. Calculated values are in arbitrary units.

To estimate the intraband contributions $\sigma_{\text{intra}}(\omega) = \Omega^2\gamma/4\pi(\omega^2 + \gamma^2)$, which fall sharply with energy (dotted lines in figure 2), the values of Ω^2 and γ were used. The values of static conductivity $\sigma_{\text{intra}}(0)$ are estimated to be 91×10^{14} s^{-1} for Sm_2Fe_{17} and 98×10^{14} s^{-1} for Tm_2Fe_{17}, correspondingly.

3. Electronic structure

Measured experimental properties of the materials can be interpreted and understood on the basis of theoretical analysis of their electronic structure. The density functional theory presents a powerful tool to do this starting from the crystal structure of a compound without other material-specific data. In this work we used the local spin-density approximation with the correction for f-electron repulsion U (LSDA + U) method [31]. As already demonstrated [22], the method allows one to reproduce collinear magnetic moments of other R_2Fe_{17} intermetallics in good agreement with experimental values, but also interpret optical conductivity in the same way as will be done in section 4.

All calculations of the electronic structure were performed in the TB-LMTO-ASA package (tight binding, linear muffin-tin orbitals, atomic sphere approximation) [32]. For the calculations we used the lattice parameters from table 1. The orbital basis included 6s, 6p, 5d and 4f muffin-tin orbitals for Sm or Tm and 4s, 4p and 3d for Fe sites. Values of direct Coulomb interaction and Hund exchange interaction necessary for LSDA + U computations from constrained LDA calculations [33] were obtained to be for the Sm 4f shell of Sm_2Fe_{17} $U_{\text{Sm}} = 5.4$ eV, $J_{\text{Sm}} = 0.60$ eV, and for the Tm 4f shell of Tm_2Fe_{17} $U_{\text{Tm}} = 4.9$ eV, $J_{\text{Tm}} = 0.76$ eV.

For Sm_2Fe_{17}, the results of our electronic structure calculations, namely, partial Fe 4p, 3d and rare-earth 5d, 4f densities of states (DOSs) for 'spin-up' (↑) and 'spin-down' (↓) projections of local spin moments, are presented in figure 3.

These DOSs are resembling the ferromagnetic fcc elemental iron: the two-peak structure of the dominating 3d states of Fe ions. Densities of Fe 4s, 4p and rare-earth 6s, 6p and 5d states are comparatively smaller. The contribution from 4f states of Sm to the total density of states

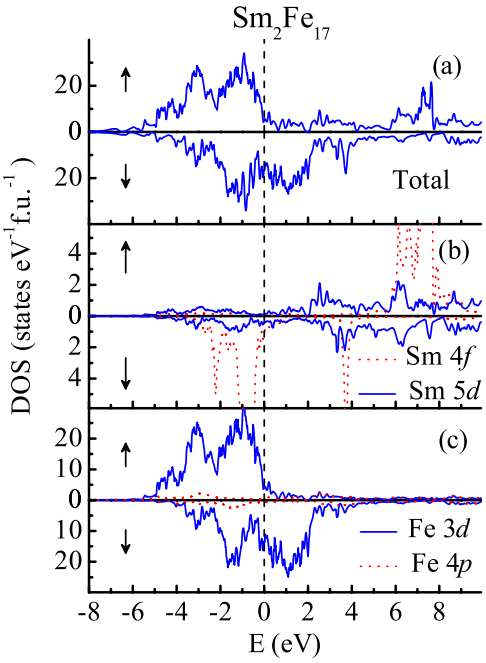

Figure 3. The densities of states for Sm_2Fe_{17}, including (a) the total density of states, (b) 4f and 5d partial densities of states for the rare-earth ion Sm and (c) 3d and 4p partial densities of states summed over all Fe ions.

Table 2. The atomic sphere radii and magnetic moments of Sm and Fe ions from the LSDA + U calculation for Sm_2Fe_{17}.

Type of ion	Atomic sphere radius (a.u.)	M (μ_B)
Sm(6c)	3.78	−5.81(−0.60[a])
Fe(6c)	2.63	2.18
Fe(9d)	2.65	2.28
Fe(18f)	2.65	2.12
Fe(18h)	2.65	2.31

[a] Corrected for the orbital magnetic moment contribution (see text).

can be seen as a two-peak band −3–0 eV and of Tm as almost filled bands just below the Fermi level from −6 to 0 eV. Empty states of the rare-earth ions are located from 3 to 9 eV for Sm and from 0 to 3 eV for Tm.

In both intermetallic compounds two solutions were found from the LSDA + U calculations: one with a ferromagnetic arrangement of Fe and Sm(Tm) sublattices and another with an antiferromagnetic one. The latter is preferred in the total energy by 0.09 Ryd for Sm_2Fe_{17} and by 0.03 Ryd for Tm_2Fe_{17}.

Magnetic moments per ion calculated in LSDA + U are presented in tables 2 and 3. Magnetic moments of the Fe ions are in good agreement with experimental data at $T = 75$ K [34] for Tm_2Fe_{17}.

Magnetic moments of the 4f shell in the rare-earth ions should be considered in detail. In all our calculations spin–orbit coupling (SOC) was neglected, since in this paper we do not address the question of magnetic anisotropy and other SOC effects. So all magnetic moments

Table 3. The atomic sphere radii and magnetic moments of Tm and Fe ions from the LSDA + U calculation and experimental neutron measurements for Tm_2Fe_{17}. The minus sign of a moment means the opposite direction to the plus sign of a moment.

Type of ion	Atomic sphere radius (a.u.)	M (μ_B)	M_{exp} (μ_B) [34]
Tm(2b)	3.05	−1.09(−6.49[a])	−6.2(2)
Tm(2d)	3.22	−1.00(−6.34[a])	−5.1(1)
Fe(4f)	2.61	2.19	2.03(6)
Fe(6g)	2.67	1.71	—
Fe(12j)	2.66	2.28	2.19(4)
Fe(12k)	2.26	1.51	1.45(4)

[a] Corrected for the orbital magnetic moment contribution (see text).

from the LSDA + U calculations are spin magnetic moments. The total magnetic moments per f.u. are equal to 26.16 μ_B for Sm_2Fe_{17} and 30.16 μ_B for Tm_2Fe_{17}. At low temperatures spin and orbital moments are collinear to each other (z axis) [34]. Hence the orbital magnetic moment increases the spin one in Tm and decreases it in the Sm ion, that results in larger/smaller ionic magnetic moment. Since experimental values of spin and orbital magnetic moments in R_2Fe_{17} compounds have not been reported, one can make a crude estimation of the total magnetic moment by including free-ionic orbital moment. Assuming pure LS coupling—hence the Landé factor g 0.286 for Sm and 1.17 for Tm—and $L = 5$ for both types of R ions, we calculate the total magnetic moment of the R ion as gJ. In iron ions the SOC is a few orders smaller than in R ions and does not affect the total magnetic moment as in R. Final values of magnetic moments for different types of R ions are shown in brackets in tables 2 and 3. This estimation imitates the major effect of SOC on the total moments in the compounds under consideration. Other effects of SOC, like formation of noncollinear magnetic structures, are not confirmed by the available experimental data, or go beyond the scope of the present investigation. There are experimental methods [35] that can help to detect spin and orbital moments in such intermetallics.

Taking into account these magnetic moments of R, the total magnetic moment of Sm_2Fe_{17} becomes 36.58 μ_B/f.u. versus the experimental one of 33.1 μ_B in the present work but perfectly match the 36.6 μ_B measured in [29]. This deviation might also be due to the varying crystal structure of the samples in the broad region of homogeneity. For Tm_2Fe_{17}, the total magnetic moment from the values in table 3 is 19.32 μ_B/f.u., that slightly differs from the experimental one of 20.4 μ_B in the present work and again is close to the 19.4 μ_B in [29]. *Ab initio* calculations properly accounting for spin–orbit coupling and strong electronic correlations on the same footing—allowing non-collinear magnetic ordering as well as non-diagonal exchange interaction terms—only very recently became possible [36]. But due to the computational efforts presented by R_2Fe_{17} they have not yet been applied to investigate these intermetallic compounds. In general we found very good agreement of theoretical and experimental total magnetic moments if the spin–orbit coupling was taken into account even in a very rough way.

4. Optical conductivity

To interpret the dispersion of the interband part of $\sigma(\omega)$ for both intermetallic systems under consideration the calculated LSDA+U band structures presented in the preceding section were used. The procedure is based on the method proposed in [37]. In order to calculate theoretical optical conductivity $\sigma_{theor}(\omega)$ we performed the convolution of the partial densities of states shown in figures 3 and 4 for each ion occupying inequivalent positions in the crystal lattice.

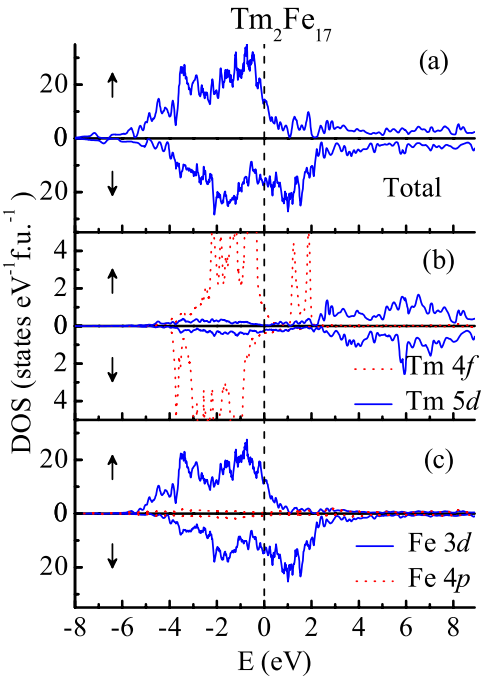

Figure 4. The densities of states for Tm_2Fe_{17}, including (a) the total density of states, (b) 4f and 5d partial densities of states for the rare-earth ion Tm and (c) 3d and 4p partial densities of states summed over all Fe ions.

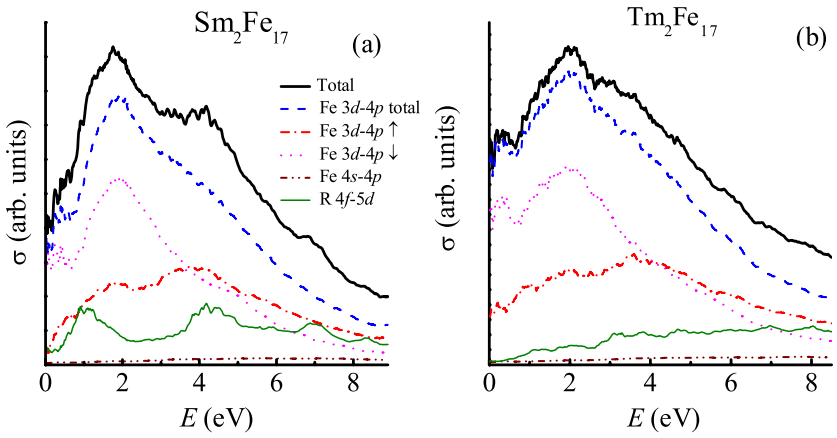

Figure 5. Calculated total and partial contributions in optical conductivity for Sm_2Fe_{17} (a) and Tm_2Fe_{17} (b) compounds. Dashed, dotted and dash–dotted lines show the total, spin-down and spin-up contributions from 3d–4p transitions in Fe ions respectively. Dash–dot–dotted lines represent the contribution from 4s–4p transitions in Fe, and thin solid lines correspond to the 4f–5d transitions in rare-earth ions. All values are in arbitrary units.

The total $\sigma_{\text{theor}}(\omega)$ is the superposition of different contributions with allowance for the dipole selection rule for orbital quantum numbers.

Corresponding conductivity curves of the optical dispersion for both compounds are shown in figures 2 and 5 as solid lines. As seen in figure 5, the biggest contribution to $\epsilon_{\text{theor}}(\omega)$

comes from 3d–4p interband optical transitions for Fe ions in the spin-down system. This kind of excitations determines a high absorption peak at ∼2 eV (dotted lines) and low-energy ascent below 1 eV. The contribution from 3d–4p transitions through the spin-up channel forms a rather broad structure with maxima at ∼3.5 eV (dash–dotted lines). For both systems, the contributions from Fe 4s–4p (dash–dot–dot lines) and Sm(Tm) 4f–5d (thin solid lines) are substantially smaller. On the whole the calculated optical properties of Sm_2Fe_{17} and Tm_2Fe_{17} are in qualitative agreement with experiment. Theoretical calculations reproduce the basic features of the $\sigma(\omega)$ spectra, namely, the sharp threshold near 1 eV, associated with the beginning of interband transitions, the width of the intense absorption band with maximum at ∼2 eV and the smooth diminution of the high-energy slope.

The appreciable resemblance of the optical conductivity spectra obtained in this work for the Sm_2Fe_{17} and Tm_2Fe_{17} compounds and published in [21, 22] for other R_2Fe_{17} systems, as well as similar behaviour of the photoemission spectra for such alloys [17], suggest that their electronic structure is qualitatively similar within few electronvolts above and below E_F. Moreover, the line shape of our $\sigma(\omega)$ is very similar to the appropriate curve for pure Fe [38]. We did not consider matrix element effects since the calculations for a prototype system, pure Fe in the fcc structure, suggest that they do not play an important role here.

5. Conclusion

In this paper the experimental results for optical properties and electronic structure calculations are presented and interpreted for Sm_2Fe_{17} and Tm_2Fe_{17}. The data demonstrate that the intermetallics are Fe-rich compounds, that predetermines a close similarity of their optical and electronic properties to a pure iron in the fcc structure. However, the inclusion of the rare-earth elements results not only in a specific crystal structure but also in varying total magnetic moment, etc. The calculated partial densities of states were used to estimate various contributions of the interband transitions to the optical conductivity, that gives good agreement with experimental curves and allows one to interpret it with respect to different optical transition contributions. Finally, despite slightly different electronic structures, Sm_2Fe_{17} and Tm_2Fe_{17} have similar optical conductivity curves, which in both cases can be understood as mainly the contribution of the 3d–4p interband transitions at the Fe ions.

Acknowledgments

This work was supported by grants of the Russian Foundation for Basic Research 05-02-17244, 05-02-16301 and 06-02-90537 and in part by programmes of the Presidium of the Russian Academy of Sciences (RAS), ‘Quantum macrophysics’, and of the Division of Physical Sciences of the RAS, ‘Strongly correlated electrons in semiconductors, metals, superconductors and magnetic materials’. Two of us (IN, AL) acknowledge the Dynasty Foundation and the International Centre for Fundamental Physics in Moscow, a grant of the President of the Russian Federation MK-2118.2005.02 (IN) and an interdisciplinary UrO-SO project (IN).

References

[1] Coey J M D 2002 *J. Magn. Magn. Mater.* **248** 441–56
[2] Buschow K H J 1997 Magnetism and processing of permanent magnet materials *Handbook of Magnetic Materials* vol 10 (Amsterdam: Elsevier) pp 463–593

[3] Duc N H 1997 Intersublattice exchange coupling in the lanthanide-transition metal intrmetallics *Handbook on the Physics and Chemistry of Rare Earths* vol 24 (Amsterdam: Elsevier) pp 369–98
[4] Gubbens P C M, Van Der Kraan A M, Jacobs T N and Buschow K H J 1990 *J. Less-Common Met.* **159** 173–8
[5] Jacobs T H, Buschow K H J, Zhou G F, Li X and de Boer F R 1992 *J. Magn. Magn. Mater.* **116** 220–30
[6] Wang Z and Dunlap R A 1993 *J. Phys.: Condens. Matter* **5** 2407–14
[7] Kuchin A G, Kourov N I, Knyazev Yu V, Kleinerman N M, Serikov V V, Ivanova G V and Ermolenko A S 1996 *Phys. Status Solidi* a **155** 479–83
[8] De Mooij D B and Buschow K H J 1988 *J. Less-Common Met.* **142** 349–57
[9] Coey J M D and Sun H 1990 *J. Magn. Magn. Mater.* **87** L251–4
[10] Sun H, Coey J M D, Otani Y and Hurley D P F 1990 *J. Phys.: Condens. Matter* **2** 6465–70
[11] Zhong X P, Radvanski R J, de Boer F R, Jacobs T H and Buschow K H J 1990 *J. Magn. Magn. Mater.* **86** 333–40
[12] Popov A G, Belozerov E V, Kuchin A G, Ermolenko A S, Makarova G M, Gaviko V S and Khrabrov V I 1990 *Phys. Status Solidi* a **121** K111–6
[13] Sun H, Akayama M, Tatami K and Fujii H 1993 *Physica* B **183** 33–9
[14] Katter M, Wecker J, Schultz L and Grossinger R 1990 *J. Magn. Magn. Mater.* **92** L14–8
[15] Mohn P and Wohlfarth E P 1987 *J. Phys. F: Met. Phys.* **17** 2421–30
[16] Jaswal S S, Yelin W B, Hadjipanayis G C, Wang Y Z and Sellmyer D J 1991 *Phys. Rev. Lett.* **67** 644–7
[17] Woods J P, Patterson B M, Fernando A S, Jaswal S S, Welipitiya D and Sellmyer D J 1995 *Phys. Rev.* B **51** 1064–72
[18] Sabirianov R F and Jaswal S S 1996 *J. Appl. Phys.* **79** 5942–4
[19] Knyazev Yu V, Kuchin A G and Kuz'min Yu I 2000 *Phys. Met. Metallogr.* **89** 558–62
[20] Knyazev Yu V, Kuchin A G and Kuz'min Yu I 2001 *J. Alloys Compounds* **327** 34–8
[21] Nekrasov I A, Knyazev Yu V, Kuz'min Yu I, Kuchin A G and Anisimov V I 2004 *Phys. Met. Metallogr.* **97** 129–32
[22] Knyazev Yu V, Lukoyanov A V, Kuz'min Yu I, Kuchin A G and Nekrasov I A 2006 *Phys. Rev.* B **73** 094410
[23] Isnard O, Miraglia S, Fruchart D, Giorgetti C, Dartyge E and Krill G 1996 *J. Phys.: Condens. Matter* **8** 2437–46
[24] Vandormael D, Grandjear F, Brious V, Middleton D P, Buschow K H J and Long G J 1997 *Phys. Rev.* B **56** 6100–6
[25] Alp E E, Umarji A M, Malik S K, Shenoy G K, Huang M Q, Boltich E B and Wallace W E 1987 *J. Magn. Magn. Mater.* **68** 305–8
[26] Li Z W, Zhou X Z and Morrish A H 1995 *Phys. Rev.* B **51** 2891–5
[27] Steinbeck L, Richter M, Nitzsche V and Eschrig H 1996 *Phys. Rev.* B **53** 7111–27
[28] Uebele P, Hummler K and Fähnle M 1996 *Phys. Rev.* B **53** 3296–303
[29] Kou X C, de Boer R R, Grossinger R, Wiesinger G, Suzuki H, Kitazawa H, Takamasu T and Kido G 1998 *J. Magn. Magn. Mater.* **177–181** 1002–7
[30] Beattie J R 1955 *Phil. Mag.* **46** 235–45
[31] Anisimov V I, Aryasetiawan F and Lichtenstein A I 1997 *J. Phys.: Condens. Matter* **9** 767–808
[32] Andersen O K 1975 *Phys. Rev.* B **12** 3060–83
[33] Gunnarsson O, Andersen O K, Jepsen O and Zaanen J 1989 *Phys. Rev.* B **39** 1708–22
[34] Park J, Jo Y, Park J-P, Prokes K, Welzel S, Lee C H, Kudrevatykh N, Valiev E, Pirogov A and Sheptyakov D 2001 *J. Magn. Magn. Mater.* **237** 158–68
[35] McCarthy J E, Duffy J A, Detlefs C, Cooper M J and Canfield P C 2000 *Phys. Rev.* B **62** R6073
[36] Shorikov A O, Lukoyanov A V, Korotin M A and Anisimov V I 2005 *Phys. Rev.* B **72** 024458
[37] Berglund C N and Spicer W E 1964 *Phys. Rev.* **136** A1030–44
Berglund C N and Spicer W E 1964 *Phys. Rev.* **136** A1044–64
[38] Kirillova M M, Knyazev Yu V and Kuz'min Yu I 1993 *Thin Solid Films* **324** 527–30